Research Article

Journal of PeptideScience

Received: 1 April 2011 Revised: 16 June 2011 Accepted: 27 June 2011 Published online in Wiley Online Library: 4 October 2011

(wileyonlinelibrary.com) DOI 10.1002/psc.1399

Inhibition of chlamydial class Ic ribonucleotide reductase by C-terminal peptides from protein R2

Maria Öhrström, Ana Popović-Bijelić†, Jinghui Luo‡, Pål Stenmark, Martin Högbom and Astrid Gräslund*

Chlamydia trachomatis **ribonucleotide reductase (RNR) is a class Ic RNR. It has two homodimeric subunits: proteins R1 and R2. Class Ic protein R2 in its most active form has a manganese–iron metal cofactor, which functions in catalysis like the tyrosyl radical in classical class Ia and Ib RNRs. Oligopeptides with the same sequence as the C-terminus of *C. trachomatis* protein R2 inhibit the catalytic activity of *C. trachomatis* RNR, showing that the class Ic enzyme shares a similar highly specific inhibition mechanism with the previously studied radical-containing class Ia and Ib RNRs. The results indicate that the catalytic mechanism of this class of RNRs with a manganese–iron cofactor is similar to that of the tyrosyl-radical-containing RNRs, involving reversible long-range radical transfer between proteins R1 and R2. The competitive binding of the inhibitory R2-derived oligopeptide blocks the transfer pathway. We have constructed three-dimensional structure models of *C. trachomatis* protein R1, based on homologous R1 crystal structures, and used them to discuss possible binding modes of the peptide to protein R1. Typical half maximal inhibitory concentration values for *C. trachomatis* RNR are about 200 μM for a 20-mer peptide, indicating a less efficient inhibition compared with those for an equally long peptide in the *Escherichia coli* class Ia RNR. A possible explanation is that the *C. trachomatis* R1/R2 complex has other important interactions, in addition to the binding mediated by the R1 interaction with the C-terminus of protein R2. Copyright © 2011 European Peptide Society and John Wiley & Sons, Ltd.**

Supporting information can be found in the online version of this article.

Keywords: class Ic ribonucleotide reductase; manganese–iron cofactor; subunit interaction inhibitor; protein R2 C-terminus; oligopeptide inhibitor

Introduction

The enzyme RNR catalyzes the conversion of all four ribonucleotides to deoxyribonucleotides, a bottleneck reaction to produce the building blocks for *de novo* DNA synthesis and repair. Class I RNRs found in eukaryotic cells and in certain bacteria are composed of subunits $\alpha 2$ and $\beta 2$. The larger $\alpha 2$ subunit R1 (typically 2×90 kDa) binds the substrate and has sites for the allosteric regulation of the enzyme, whereas the smaller $\beta 2$ subunit R2 (typically 2×45 kDa) in each polypeptide chain normally carries a dinuclear metal cluster and a stable free radical on a neighboring tyrosyl residue [1]. The radical is required for enzyme activity, which involves long-range electron transfer between the R1 and R2 subunits [2–4].

The question of which metal ions are involved in RNR activity in different species has recently become a hot and debated topic. Besides the well-studied class Ia iron enzymes, recent reports provide evidence of the involvement of manganese in certain bacterial RNRs. In *Escherichia coli* [5] and *Corynebacterium ammoniagenes* [6] class Ib enzymes, a dimanganese cluster can give rise to the catalytically active tyrosyl radical, and in class Ic, prototyped by the chlamydial enzymes, a mixed manganese–iron cluster without amino-acid-based free radical can initiate the catalytic reaction [7,8]. Hence, the RNR subclasses Ia, b and c, which have mainly been defined from comparisons of sequence and allosteric regulation [1,9], may turn out to be differentiated also by their metal requirements for efficient catalysis.

Class Ic RNR was discovered in *Chlamydia trachomatis*. The reported crystal structure of *C. trachomatis* RNR R2 protein revealed that the dimetal site displays significant differences compared with class Ia and Ib R2s [9]. It also has a phenylalanine residue at the position of the conserved radical-harboring tyrosine. It was shown that *C. trachomatis* protein R2 can bind a manganese ion in place of one iron ion and form a mixed-metal Mn–Fe cluster [7,8] and that the Mn/Fe-containing wild-type R2 protein shows considerably higher specific activity (at least sixfold) than its Fe-only counterpart [8]. Although the enzymatic activity of the Fe-only form of the class Ic RNR R2 is controversial [7,8], it seems to require activation by metal ion reduction and

* *Correspondence to: Astrid Gräslund, Department of Biochemistry and Biophysics, The Arrhenius Laboratories for Natural Sciences, Stockholm University, SE-106 91 Stockholm, Sweden. E-mail: astrid@dbb.su.se*

Department of Biochemistry and Biophysics, Stockholm University, SE-10691 Stockholm, Sweden

† *Current address: Faculty of Physical Chemistry, University of Belgrade, 11158 Belgrade, Serbia.*

‡ *Current address: Leiden Institute of Chemistry, Leiden University, 2300 RA Leiden, The Netherlands.*

Abbreviations used: RNR, ribonucleotide reductase; HSV, herpes simplex virus; ATP, adenosine 5′-triphosphate; CDP, cytidine 5′-diphosphate; DTT, dithiothreitol.

Journal of PeptideScience

reaction with molecular oxygen for each catalytic cycle [10]. Enzyme activity measurements and Mössbauer spectroscopy have indicated that *C. trachomatis* RNR uses a stable Mn(IV)–Fe(III) cofactor in protein R2 for activity. This redox active state is formed from a reaction of the reduced metal cluster with molecular oxygen to initiate the formation of the cysteinyl free radical after substrate binding in protein R1 [7]. Density functional theory calculations have supported the idea that the Mn(IV) ion of the Mn(IV)–Fe(III) cofactor is an equally strong oxidant as the tyrosyl radical in class Ia *E. coli* R2 protein [11], thereby suggesting an explanation for the reversible electron transfer in multiple catalytic cycles also in this enzyme class. Genomic analyses suggest that over 50 organisms contain class Ic R2 proteins [12]. Pathogens are common in this group, emphasizing the importance of inhibition studies of the class Ic.

In the manganese-only class Ib RNRs, on the other hand, a reduced dimanganese cluster appears to react with two partly reduced oxygen molecules (suggested to be HO_2^- produced by an unusual flavodoxin NrdI bound to R2) to form a neighboring tyrosyl radical [5,6]. Whether this process is functional in all native class Ib enzymes and whether it depends on the availability of suitable metal ions under different conditions remain to be determined [13].

Despite the obviously different metal binding properties, the class I R1 and R2 proteins are closely related in molecular structure between the three subclasses. For class Ia and Ib, it is known that oligopeptides with sequences derived from the C-terminus of the respective R2 protein are efficient and specific inhibitors of enzyme activity [14]. Their inhibitory activity is based on competitive binding to the R1/R2 interaction area of R1, thereby blocking the formation of a catalytically active R1/R2 complex. Such oligopeptides have also been found to be useful for crystallization of the R1 protein and have been found at particular binding sites in the crystal structures of the R1 proteins of, e.g. *E. coli* RNR [15] and *Saccharomyces cerevisiae* RNR [16].

In the present study, we have investigated the inhibitory effect of R2 C-terminal oligopeptides on *C. trachomatis* class Ic RNR. We have made a model of the *C. trachomatis* R1 protein based on the published structure of yeast protein R1 [16] and have used this model to suggest a likely binding area for the peptide and to discuss possible binding modes. Besides the obvious importance of defining potential inhibitory agents acting on a potent and common pathogen, our results also suggest that the catalytic mechanism of the class Ic RNRs with a manganese–iron cofactor and without an amino-acid-based free radical is in essence identical to that of the tyrosyl-radical-containing RNRs, involving reversible long-range radical transfer between proteins R1 and R2. This transfer pathway is blocked by the competitive binding of the inhibitory peptide.

Materials and Methods

Molecular Modeling

The protein structure homology-modeling server Swiss-Model was used to generate homology models of the *C. trachomatis* R1 protein [17]. Two models were generated, one using the yeast structure as template (PDB id: 1ZYZ) and one using the human structure as template (PDB id: 2WGH), resulting in qualitatively very similar models. Other modeling servers were also tried, and the results were virtually identical. Figures were generated using Pymol (www.pymol.org), and the alignment figure was generated using ESPript [18]. The yeast and *E. coli* R2 peptides were positioned by superpositioning the *C. trachomatis* model with the R2 peptide complexes of *E. coli* (PDB id: 3R1R) and yeast (PDB id: 2CVY).

Materials

For the preparation of lysogeny broth (LB) and terrific broth media, Bacto Tryptone and yeast extract were purchased from Becton, Dickinson and Co. (Le Pont de Claix, France). [^{3}H]CDP was purchased from Amersham Pharmacia Biotech (Amersham, UK). Oligopeptides of different lengths were synthesized by PolyPeptide Laboratories (Strasbourg, France).

Expression and Purification of RNR Proteins

Plasmids encoding overexpression of *C. trachomatis* wild-type R2 and truncated wild-type R1 proteins, pET3a-R2 and pET3a-CTR1Δ1-248, respectively, were constructed in the laboratory of Grant McClarty, University of Manitoba, Canada, and were received as a kind gift from him. The truncated R1Δ1-248 protein was selected instead of the full-length R1 protein on the basis of its better stability, higher yield and almost identical behavior in activity experiments [19].

The bacterial cultures were grown overnight in LB medium, pH 7.5, with 27.2 μg ml^{-1} chloramphenicol and 50 μg ml^{-1} carbenicillin at 37 °C. Six flasks with 800 ml of LB (terrific broth for R1 protein) medium, containing the same antibiotic concentration, were inoculated with 7 ml of the overnight culture and shaken vigorously at 37 °C. When the culture reached $A_{595} = 0.8$, the temperature was reduced to 15 °C, and the protein expression was initiated with isopropyl β-D-1-thiogalactopyranoside at a final concentration of 500 μM. The cultures were grown overnight for about 15 h at 15 °C. Coincident with the isopropyl β-D-1-thiogalactopyranoside addition, $MnCl_2$ was added to a final concentration of 30 μM to the R2-protein-containing cultures. *C. trachomatis* RNR proteins were purified essentially as reported in [19] and [8] and briefly described in the succeeding paragraphs.

Approximately 15 h after induction, the cultures were chilled and harvested by centrifugation at 4000 rpm for 20 min at 4 °C. The cell pellets were resuspended in 50 mM Tris/HCl, 200 mM KCl buffer (pH 7.6), quickly frozen in liquid nitrogen and stored at −80 °C.

The frozen bacteria were gently thawed in a 25 °C water bath and centrifuged at 45 000 rpm for 30 min at 4 °C. Nucleic acids were removed by precipitation with streptomycin sulfate to a final concentration of 10%, and the solution was cleared by centrifugation at 15 000 rpm for 20 min at 4 °C. The proteins were then precipitated with 40% ammonium sulfate and collected by centrifugation at 15 000 rpm for 20 min at 4 °C. The pellets were gently resuspended in milliliter volumes of 50 mM Tris/HCl, pH 7.6, desalted over a column containing Sephadex G-25 medium (Amersham Pharmacia Biotech) and then applied to a column of diethylaminoethyl cellulose (DE52, Whatman, Maidstone, UK) previously equilibrated with 20 mM Tris/HCl, pH 7.6, 60 mM NaCl. The column was washed with 12 ml of the same buffer, and then the protein was eluted with 20 mM Tris/HCl, pH 7.6, 120 mM NaCl.

R1/R2-containing fractions were pooled and concentrated by centrifugation using Millipore (Billerica, MA, USA) concentrators

(50 000 molecular weight cut-off (MWCO) for R1 and 30 000 MWCO for R2) at 4000 rpm for 30 min at 4 °C. The protein was frozen in liquid nitrogen and stored at −80 °C.

Protein purity was analyzed by sodium dodecyl sulfate polyacrylamide gel electrophoresis. The protein concentrations were determined spectrophotometrically by measuring the absorbance at 280 nm. Protein concentration was calculated using the molar extinction coefficients at 280 nm for monomeric polypeptides, 138 660 $M^{-1} cm^{-1}$ for *C. trachomatis* protein R1 and 57 750 $M^{-1} cm^{-1}$ for *C. trachomatis* protein R2 [7].

Enzyme Activity Assay

C. trachomatis protein R2 activity was determined by measuring the reduction of [^{3}H]CDP in the presence of an excess of *C. trachomatis* protein R1Δ1-248 as described earlier [20]. In the assay mixture of a final volume of 50 µl, 4 mM Hepes buffer, pH 7.5, 10 mM KCl, 10 mM $MgCl_2$, 0.01 mM $FeCl_3$, 1.5 mM ATP, 10 mM DTT, 0.5 mM [^{3}H]CDP (specific activity 12 000 cpm $nmol^{-1}$), 2 µM protein R2 and 10 µM protein R1Δ1-248 were incubated for 20 min at 37 °C. For the inhibition experiments, the different peptides were dissolved in 50 mM Hepes buffer, pH 7.5, at about 1–10 mg ml^{-1}, and appropriate amounts were added to the assay mixture. The enzyme activity was measured with concentrations of the peptides up to 3 mM, when the enzyme activity was completely abolished. Each experiment was repeated at least two times. In a typical experiment, protein R1 was first added to the assay mixture, followed by inhibitory peptide. After this, the sample was left on ice for approximately 10 min, before incubation with protein R2 at 37 °C.

Enzyme-specific activity is expressed in nanomole per minute per milligram. One unit of specific enzyme activity is defined as 1 nmol of dCDP formed per minute per milligram R2 under standard conditions and in the presence of excess protein R1.

Metal Content Determination

The manganese concentration of *C. trachomatis* protein R2 was determined in acid-denatured protein by electron paramagnetic resonance spectroscopy at 293 K with a microwave power of 3 mW and modulation amplitude of 1 mT. The concentration of manganese was determined by comparing the amplitude of the electron paramagnetic resonance signal with a standard solution of 0.5 mM $MnCl_2$ as described in [21]. The iron content was spectrophotometrically determined using an iron/total iron binding capacity (ferrozine) reagent set from Eagle Diagnostics (Cedar Hill, TX, USA).

Results

Protein R1 Structure Model

The oligopeptides with sequences corresponding to the C-terminus of protein R2 are likely to inhibit the enzyme because of competitive binding to protein R1. Indeed, the crystallization of protein R1 from various species has required the presence of this type of R2-derived peptides, which are also visible in the respective crystal structures of protein R1. In the absence of a determined three-dimensional structure of the *C. trachomatis* protein R1, we constructed model structures of *C. trachomatis* R1 based on the known structures of the yeast *S. cerevisiae* and human R1 proteins (PDB id: 1ZYZ and 2WGH, respectively) [16,22]. Both yeast and human proteins have 37% sequence identity with *C. trachomatis* R1, and both model structures are very similar. Figure 1 shows the model based on the yeast R1 structure. The N-terminal 248 amino acids are not included in the R1 construct used in the experimental part of the present study. It is clear from this structure model that the omitted N-terminal domain is located on the opposite side of the protein, relative to the R2 peptide interaction area (Figure 1). It is therefore unlikely that the absence of this domain influences the peptide binding properties of the protein. An alignment of the amino acid sequences of *C. trachomatis* class Ic R1 and the class Ia R1s from yeast, *Homo sapiens* and *E. coli*, starting from *C. trachomatis* R1 residue 249 is shown in Supporting Information Figure S1.

Preparation of RNR Proteins: Metal Content of the R2 Protein

The recombinant *C. trachomatis* RNR proteins R1 and R2 were produced in *E. coli*. The R2 protein was purified from bacterial cells grown in the manganese-enriched LB medium (concentration of Mn was 30 µM and Fe was 8 µM). The proteins were assayed without further treatment or addition of metal ions. The metal content of the purified *C. trachomatis* R2 protein was determined to be 0.45 ± 0.02 Mn/polypeptide and 1.45 ± 0.02 Fe/polypeptide, in general agreement with previous enzyme preparation using the same procedures [8,10,21]. It has previously been shown that the catalytic activity of *C. trachomatis* is dependent on the amount of incorporated Mn/Fe in its R2 component. A total of two metal ions per polypeptide distributed in a 1 : 1 Mn : Fe ratio should give the maximum activity [7]. This metal uptake, and corresponding high activity, is however not possible to obtain under standard rich-medium growth conditions, even when supplemented with manganese, but a procedure including the reconstitution of the R2 apoprotein is necessary. In another study, it was shown that *E. coli* cells expressing recombinant *C. trachomatis* R2 grown in the normal LB medium incorporate at least 10 times less Mn than Fe and that the cells grown in the Mn-enriched LB medium incorporate up to 0.45 Mn/polypeptide [10]. The activities reported in the latter case were considerably lower than in [7]. In the present study, we have used the method of growing cells in the Mn-enriched LB medium, hence the more modest activity.

Inhibition of Enzyme Activity by Oligopeptides

The RNR enzyme activity was determined from the amount of product formed from the radioactively labeled substrate [^{3}H]CDP. The inhibition of the RNR catalytic activity by the addition of any of the six synthetic peptides corresponding to varying lengths and sequences of the C-terminal end of *C. trachomatis* R2 was studied under identical experimental conditions. The peptide sequences, acetylated at the N-terminus, are shown in Table 1. Peptides 1–4 have sequences corresponding to the C-terminal end of *C. trachomatis* R2. Peptides 5–6 lack the C-terminal tryptophan, and in addition, peptide 6 has one altered amino acid in its sequence (isoleucine replaced by threonine). The inhibitory activities of the synthetic peptides were determined using the described RNR activity assay [20]. Figure 2 shows the specific activity of the *C. trachomatis* protein R2 in the presence of the inhibitory 12-mer, the Ac-VIEYQHAASLTW peptide. The assay mixture that contained 4 mM Hepes buffer, pH 7.5, 10 mM KCl, 10 mM $MgCl_2$, 0.01 mM $FeCl_3$, 1.5 mM ATP, 10 mM DTT, 0.5 mM [^{3}H]CDP, 2 µM *C. trachomatis* protein R2, 10 µM

Journal of PeptideScience

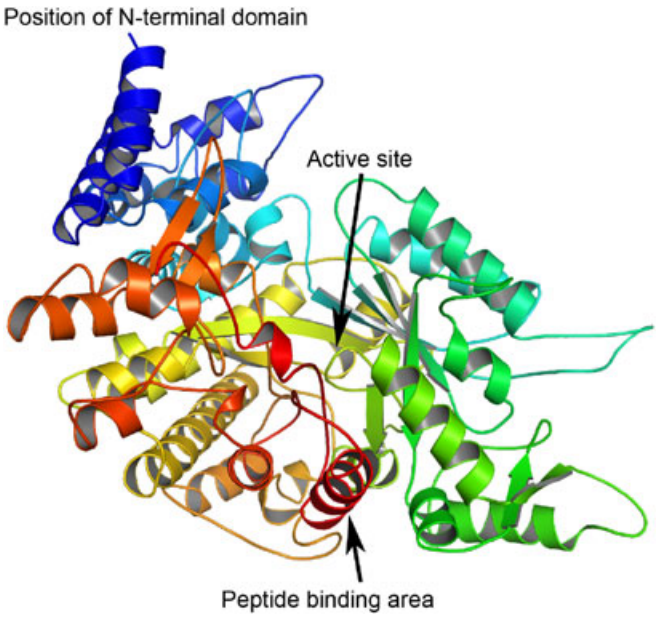

Figure 1. A ribbon representation of the *C. trachomatis* R1 model, based on the yeast R1 structure (PDB id: 1ZYZ). The structure is shown in a rainbow color representation, from the N-terminus (blue) to the C-terminus (red). The position of the peptide binding area, the active site and the position of N-terminal domain are indicated.

C. trachomatis protein R1 and various concentrations of the Ac-VIEYQHAASLTW peptide was incubated for 20 min at 37 °C. The inhibitory activity of this peptide was found to be independent of the order of addition of protein R2 and inhibitory peptide, implying that the results are independent of whether the R1–peptide complex or the R1–R2 complex was allowed to form first (data not shown). A typical specific activity in the absence of the inhibitory peptides was about 130 nmol min^{-1} mg^{-1}. The enzyme activity as a function of oligopeptide concentration follows approximately a sigmoid curve (Figure 2), as observed previously for HSV RNR [23]. From the parameters of the fitted curve, a half maximal inhibitory concentration (IC_{50}) value, i.e. the peptide concentration for which the activity is decreased by 50%, was determined. Similar inhibition experiments were performed also for the other *C. trachomatis* peptide sequences of varying lengths (data not shown). From these experiments, the IC_{50} values were estimated for the *C. trachomatis* peptides and are included in Table 1.

Table 1. The IC_{50} values of inhibitory peptides derived from the C-terminal sequence of *C. trachomatis* RNR R2 protein

Peptide sequence	IC_{50} (μM)
Ac-H**AA***S**L**T**W*	600 ± 80
Ac-**VI***E*Y*Q*H**AA***S**L**T**W*	450 ± 60
Ac-E*K**N***FF***E***T**R***VI***E*Y*Q*H**AA***S**L**T**W*	190 ± 30
Ac-*MSE**T***I***D***L***N***K***E***K***N***FF***E***T**R***VI***E*Y*Q*H**AA***S**L**T**W*	350 ± 50
Ac-E*Y*Q*H**AA***S**L**T*	>2000
Ac-**V***T*E*Y*Q*H**AA***S**L**T*	2000 ± 150

Amino acid representation: hydrophobic (bold), polar (italic), charged (underlined) and unique (normal font).

Discussion

The results presented here show that oligopeptides (the first four in Table 1) corresponding exactly to the R2 C-terminal sequences are able to inhibit the *C. trachomatis* RNR reaction, using recombinant *C. trachomatis* R2 protein produced under conditions to incorporate manganese (and iron) in the R2 metal cluster. We conclude that the inhibition mechanism that has been shown for class Ia and Ib RNR also operates for *C. trachomatis* class Ic RNR. The inhibition potency increases up to a peptide length of about 20 residues. It is also worth noting that peptides lacking the last C-terminal residue (peptides 5–6 in Table 1) are only weak inhibitors, indicating that the presence of this residue, a tryptophan in *C. trachomatis* R2, is very important for the inhibitory effect of the R2 peptide. It should also be noticed that the inhibitory activity of the C-terminal peptide suggests that the manganese–iron-containing RNRs without tyrosyl radical operate with the same mechanism of long-range proton-coupled electron transfer that has been shown for the RNRs with tyrosyl radical. These results are in agreement with those presented in the recent study of hydroxyurea inhibition of the *C. trachomatis* RNR by the Bollinger/Krebs group [24], where the two conserved residues W51 and Y338 in protein R2 were discussed as partners in the electron transfer involved in the catalytic process.

The results presented here also show that the *C. trachomatis*-derived C-terminal R2 peptides are less efficient inhibitors compared with the other RNRs [14]. A hypothetic explanation could be that the R1/R2 interaction in the *C. trachomatis* case is based to a larger extent on other interactions than the R2–C-terminus interaction.

The three-dimensional structures of *E. coli* and yeast R1 proteins have been determined, in complex with their respective R2 peptides, by X-ray crystallography [15,16]. Figure 3A, B shows the electrostatic surface potential of the relevant areas of the *E. coli* and yeast R1 proteins. Both peptides bind in the same general position on the R1 surface but with different, almost perpendicular, orientations [25]. Figure 3C, D shows the surface potential of the same area of the *C. trachomatis* protein R1 model.

The 12 C-terminal residues of *E. coli* R2 peptide bind in a cleft between α13 (N340–E351, *E. coli* numbering) and αI

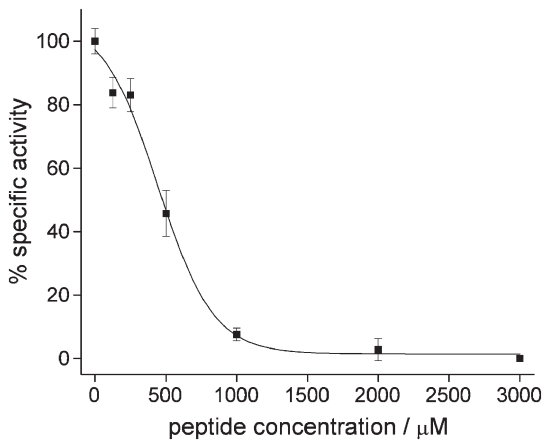

Figure 2. *C. trachomatis*-R2-specific activity as a function of inhibitory peptide concentration, obtained for the Ac-VIEYQHAASLTW peptide. The assay was performed in 4 mM Hepes buffer, pH 7.5, with 10 mM KCl, 10 mM $MgCl_2$, 0.01 mM $FeCl_3$, 1.5 mM ATP, 10 mM DTT, 0.5 mM [^{3}H]CDP, 2 μM protein R2 and 10 μM protein R1Δ1-248. The solutions were incubated for 20 min at 37 °C. The inhibitory peptide was dissolved in 50 mM Hepes buffer, pH 7.5.

(M711–F724, *E. coli* numbering) helices [15]. Pender *et al*. [26] suggested that in a number of prokaryotic and eukaryotic species the binding site for the seven C-terminal residues of R2 is defined by *E. coli* R1 residues (*E. coli* numbering) Y344, T345, L348, L719, Y722 and K723 (see Supporting Information Figure S2). These R1 residues are to some extent conserved, particularly among prokaryotes. The corresponding residues in *C. trachomatis* R1 are F577, K578, Q581, L979, W982 and K983 (*C. trachomatis* numbering, see Supporting Information Figure S1). These residues are indicated in Figure 3C. Figure 3D compares the positioning of the *E. coli* and yeast peptides on the modeled *C. trachomatis* R1 structure. We observe that the electrostatic interaction with a bound peptide oriented like the yeast peptide would be unfavorable because of electrostatic repulsion between negatively charged side chains of *C. trachomatis* R1 and the C-terminal carboxyl of the R2 peptide (Supporting Information Figure S1). There are no apparent features that would preclude a binding mode of the *C. trachomatis* peptide similar to the one found in the *E. coli* R1/R2 peptide complex, although the details of the interaction and binding may be different from those in both the *E. coli* and yeast systems. Attempts to better define the binding site by theoretical docking studies were inconclusive because they could not properly predict the two experimentally determined complex structures of *E. coli* and yeast R1 with their respective peptides (data not shown).

The C-terminal inhibitory peptide sequences of some class I RNRs are shown in Table 2. An interesting aspect of these peptide sequences is that the hydrophobic matching between the R2 peptides and the binding area on R1 seems to be a very important factor for the interaction [26]. The negatively charged residues in most systems (Table 2) have little correspondence in *C. trachomatis* R2, which instead has a few polar residues present in its C-terminus. In the crystal structures of *E. coli* and yeast R1, the side chains of those residues do not interact with protein R1. The role of these polar/charged residues may instead be to keep the C-terminal end soluble and ready to interact with a suitable partner.

RNR inhibitors of class Ia and Ib enzymes may be grouped according to their specific modes of action [32]. They can be divided into three broad groups: translation inhibitors, which stop enzyme synthesis; interaction inhibitors, which block the formation of the R1/R2 holoenzyme; and catalytic inhibitors, which react with the active state of RNR. Among these groups, the most

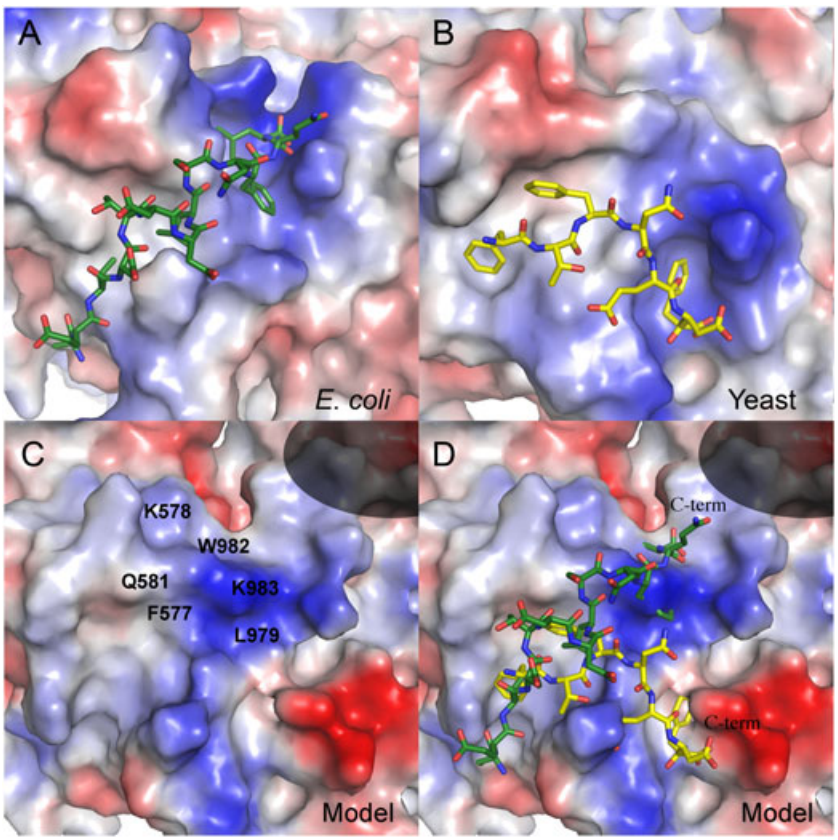

Figure 3. Surface charge representations of the *E. coli* (A), yeast (B) and modeled *C. trachomatis* R1 (C, D), showing the same surface area according to superpositioning of the three-dimensional structures. A: Structure of *E. coli* R1 in complex with *E. coli* R2 peptide (PDB id: 3R1R). The very C-terminus of the R2 peptide is located in the upper right corner. The surface contact potential shows hydrophobic interactions as well as a positively charged patch interacting with the C-terminal main-chain carboxyl of the peptide. B: Structure of yeast R1 in complex with yeast R2 peptide (PDB id: 2CVY). The C-terminus of the R2 peptide is located in the lower right corner. The surface contact potential shows hydrophobic interactions and a similar charged interaction with the C-terminal main-chain carboxyl of the peptide. C: Location of residues proposed to form part of the peptide binding site (see text) in the *C. trachomatis* structure model. D: Both R2 peptides overlaid on the surface of a model of the *C. trachomatis* R1. The surface contributed by an insertion in the *C. trachomatis* R1 protein (and thus very uncertain) is indicated in gray. The model *C. trachomatis* surface contact potential appears qualitatively more similar to the *E. coli* surface compared with the yeast surface. The surface potential of the *C. trachomatis* R1 model suggests that the binding mode observed in the yeast system would be unfavorable because of electrostatic repulsion to the R2 C-terminal main-chain carboxyl. The large differences in the binding modes between the *E. coli* and yeast peptides also suggest that the interaction is not conserved and that the *C. trachomatis* R2 peptide may interact with R1 in a mode different from both *E. coli* and yeast.

Journal of PeptideScience

Table 2. C-terminal inhibitory peptide sequences of some class I RNRs

Origin	Inhibitory peptide
C. trachomatis	EK*N***FF**E*T*R**VI**E**Y**Q*H***AA***S***L***T***W**[a]
E. coli	**YLV**G*Q***I**D*S*E**V**D*T*D**D**L*S**N***FQ***L**[b]
Mouse	**F***T***L**D**A**D**F**[c]
M. tuberculosis	EDDD**W**D**F**[d]
S. cerevisiae	**F***T***F***N*ED**F**[e]
Herpes simplex virus	**YA**G**AVV***N***D**L[f]

Amino acid representation: hydrophobic (bold), polar (italic), charged (underlined) and unique (normal font).

[a]From this work.

[b]From [27].

[c]From [28].

[d]From [29].

[e]From [30].

[f]From [31].

specific inhibitors are the interaction inhibitors. The specificity of oligopeptide inhibitors was first demonstrated for a nonapeptide that inhibited the HSV RNR without affecting the activity of the mammalian enzyme [23,31,33]. Efficient inhibition by R2 C-terminal peptides has later been demonstrated for class Ia *E. coli* [27], mammalian [28,34] and *S. cerevisiae* [30] RNRs among others, as reviewed in [14], and also for the pathogenic *Mycobacterium tuberculosis* class Ib RNR [29,35,36]. It can now be concluded that the Mn/Fe-cofactor-containing class Ic RNRs will follow the same pattern of oligonucleotide inhibition of the catalytic process. This type of peptides remains a good starting point for constructing species-specific inhibitors to RNR for pharmaceutical purposes.

Acknowledgements

This work was supported by grants from the Wenner-Gren Foundations, the Swedish Foundation for Strategic Research, the Center for Biomembrane Research and the Swedish Research Council.

Supporting information

Supporting information can be found in the online version of this article.

References

1 Reichard P. From RNA to DNA, why so many ribonucleotide reductases? *Science* 1993; **260**: 1773–1777.
2 Nordlund P, Eklund H. Structure and function of the *Escherichia coli* ribonucleotide reductase protein R2. *J. Mol. Biol.* 1993; **232**: 123–146.
3 Uhlin U, Eklund H. The structure of ribonucleotide reductase protein R1. *Nature* 1994; **370**: 533–539.
4 Stubbe J, Nocera DG, Yee CS, Chang MCY. Radical initiation in the class I ribonucleotide reductase: long range proton-coupled electron transfer? *Chem. Rev.* 2003; **103**: 2167–2202.
5 Cotruvo JA, Stubbe J. An active dimanganese(III)-tyrosyl radical cofactor in *Escherichia coli* class Ib ribonucleotide reductase. *Biochemistry* 2010; **49**: 1297–1309.
6 Cox N, Ogata H, Stolle P, Reijerse E, Auling G, Lubitz W. A tyrosyldimanganese coupled spin system is the native metalloradical cofactor of the R2F subunit of the ribonucleotide reductase of *Corynebacterium ammoniagenes*. *J. Am. Chem. Soc.* 2010; **132**: 11197–11213.
7 Jiang W, Yun D, Saleh L, Barr EW, Xing G, Hoffart LM, Maslak MA, Krebs C, Bollinger JM Jr. A manganese(IV)/iron(III) cofactor in *Chlamydia trachomatis* ribonucleotide reductase. *Science* 2007; **316**: 1188–1191.
8 Voevodskaya N, Lendzian F, Ehrenberg A, Gräslund A. High catalytic activity achieved with a mixed manganese–iron site in protein R2 of *Chlamydia* ribonucleotide reductase. *FEBS Lett.* 2007; **581**: 3351–3355.
9 Högbom M, Stenmark P, Voevodskaya N, McClarty G, Gräslund A, Nordlund P. The radical site in *Chlamydia* ribonucleotide reductase defines a new R2 subclass. *Science* 2004; **305**: 245–248.
10 Popović-Bijelić A, Voevodskaya N, Domkin V, Thelander L, Gräslund A. Metal binding and activity of ribonucleotide reductase protein R2 mutants: conditions for formation of the mixed manganese–iron cofactor. *Biochemistry* 2009; **48**: 6532–6539.
11 Roos K, Siegbahn PEM. Density functional study of the manganese-containing ribonucleotide reductase from *Chlamydia trachomatis*: why manganese is needed in the active complex. *Biochemistry* 2009; **48**: 1878–1887.
12 Högbom M. The manganese/iron-carboxylate proteins: what is what, where are they, and what can the sequences tell us? *J. Biol. Inorg. Chem.* 2010; **15**: 339–349.
13 Högbom M. Metal use in ribonucleotide reductase R2, di-iron, di-manganese and heterodinuclear—an intricate bioinorganic workaround to use different metals for the same reaction. *Metallomics* 2011; **3**: 110–120.
14 Cooperman B. Oligopeptide inhibition of class I ribonucleotide reductases. *Biopolymers* 2003; **71**: 117–131.
15 Uhlin U, Uhlin T, Eklund H. Crystallization and crystallographic investigations of the ribonucleotide reductase protein R1 from *Escherichia coli*. *FEBS Lett.* 1993; **336**: 148–152.
16 Xu H, Faber C, Uchiki T, Racca J, Dealwis C. Structures of eukaryotic ribonucleotide reductase I provide insights into dNTP regulation. *Proc. Natl. Acad. Sci. U. S. A.* 2006; **103**: 4022–4027.
17 Arnold K, Bordoli L, Kopp J, Schwede T. The SWISS-MODEL workspace: a Web-based environment for protein structure homology modeling. *Bioinformatics* 2006; **22**: 195–201.
18 Gouet P, Robert X, Courcelle E. ESPript/ENDscript: extracting and rendering sequence and 3D information from atomic structures of proteins. *Nucleic Acids Res.* 2003; **31**: 3320–3323.
19 Roshick C, Iliffe-Lee ER, McClarty G. Cloning and characterization of ribonucleotide reductase from *Chlamydia trachomatis*. *J. Biol. Chem.* 2000; **275**: 38111–38119.
20 Engström Y, Eriksson S, Thelander L, Akerman M. Ribonucleotide reductase from calf thymus. Purification and properties. *Biochemistry* 1979; **18**: 2941–2948.
21 Voevodskaya N, Lendzian F, Sanganas O, Grundmeier A, Gräslund A, Haumann M. Redox intermediates of the Mn–Fe site in subunit R2 of *Chlamydia trachomatis* ribonucleotide reductase. An X-ray absorption and EPR study. *J. Biol. Chem.* 2009; **284**: 4555–4566.
22 Welin M, Nordlund P. Understanding specificity in metabolic pathways—structural biology of human nucleotide metabolism. *Biochem. Biophys. Res. Commun.* 2010; **396**: 157–163.
23 Gaudreau P, Michaud J, Cohen EA, Langelier Y, Brazeau P. Structure–activity studies on synthetic peptides inhibiting herpes simplex virus ribonucleotide reductase. *J. Biol. Chem.* 1987; **262**: 12413–12416.
24 Jiang W, Xie J, Varano PT, Krebs C, Bollinger JM Jr. Two distinct mechanisms of inactivation of the class Ic ribonucleotide reductase from *Chlamydia trachomatis* by hydroxyurea: implications for the protein gating of intersubunit electron transfer. *Biochemistry* 2010; **49**: 5340–5349.
25 Xu H, Faber C, Uchiki T, Racca J, Dealwis C. Structures of eukaryotic ribonucleotide reductase I define gemcitabine diphosphate binding and subunit assembly. *Proc. Natl. Acad. Sci. U. S. A.* 2006; **103**: 4028–4033.
26 Pender B, Wu X, Axelsen P, Cooperman BS. Toward a rational design of peptide inhibitors of ribonucleotide reductase: structure–function and modeling studies. *J. Med. Chem.* 2001; **44**: 36–46.
27 Climent I, Sjöberg BM, Huang CY. Carboxyl-terminal peptides as probes for *Escherichia coli* ribonucleotide reductase subunit interaction: kinetic analysis of inhibition studies. *Biochemistry* 1991; **30**: 5164–5171.
28 Yang FD, Spanevello RA, Celiker I, Hirschmann R, Rubin H, Cooperman BS. The carboxyl terminus heptapeptide of the R2 subunit of

mammalian ribonucleotide reductase inhibits enzyme activity and can be used to purify the R1 subunit. *FEBS Lett.* 1990; **272**: 61–64.

29 Yang F, Curran SC, Li LS, Avarbock D, Graf JD, Chua MM, Lu G, Salem J, Rubin H. Characterization of two genes encoding the *Mycobacterium tuberculosis* ribonucleotide reductase small subunit. *J. Bacteriol.* 1997; **179**: 6408–6415.

30 Fisher A, Yang FD, Rubin H, Cooperman BS. R2 C-terminal peptide inhibition of mammalian and yeast ribonucleotide reductase. *J. Med. Chem.* 1993; **36**: 3859–3862.

31 Cohen EA, Gaudreau P, Brazeau P, Langelier Y. Specific inhibition of herpesvirus ribonucleotide reductase by a nonapeptide derived from the carboxy terminus of subunit 2. *Nature (London)* 1986; **321**: 441–443.

32 Cerqueira NM, Pereira S, Fernandes PA, Ramos MJ. Overview of ribonucleotide reductase inhibitors: an appealing target in anti-tumour therapy. *Curr. Med. Chem.* 2005; **12**: 1283–1294.

33 Dutia BM, Frame MC, Subak-Sharpe JH, Clark WN, Marsden HS. Specific inhibition of herpesvirus ribonucleotide reductase by synthetic peptides. *Nature (London)* 1986; **321**: 439–441.

34 Cosentino G, Lavallée P, Rakhit S, Plante R, Gaudette Y, Lawetz C, Whitehead PW, Duceppe JS, Lépine-Frenette C, Dansereau N, Guilbalt C, Langelier Y, Gaudreau P, Thelander L, Guindon Y. Specific inhibition of ribonucleotide reductases by peptides corresponding to the C-terminal of their second subunit. *Biochem. Cell Biol.* 1991; **69**: 79–83.

35 Nurbo J, Roos AK, Muthas D, Wahlström E, Ericsson DJ, Lundstedt T, Unge T, Karlén A. Design, synthesis and evaluation of peptide inhibitors of *Mycobacterium tuberculosis* ribonucleotide reductase. *J. Pept. Sci.* 2007; **13**: 822–832.

36 Ericsson DJ, Nurbo J, Muthas D, Hertzberg K, Lindeberg G, Karlén A, Unge T. Identification of small peptides mimicking the R2 C-terminus of *Mycobacterium tuberculosis* ribonucleotide reductase. *J. Pept. Sci.* 2010; **16**: 159–164.

